A New Route toward Ultrasensitive, Flexible Chemical Sensors: Metal Nanotubes by Wet-Chemical Synthesis along Sacrificial Nanowire Templates
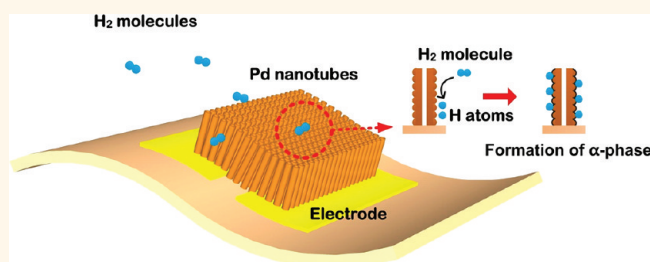
Mi Ae Lim,[†,¶] Dong Hwan Kim,[†,¶] Chong-Ook Park,[‡] Young Wook Lee,[§] Sang Woo Han,[§] Zhiyong Li,[⊥] R. Stan Williams,[⊥] and Inkyu Park[†,*]

[†]Department of Mechanical Engineering & KI for the NanoCentury, [‡]Department of Materials Science and Engineering, and [§]Department of Chemistry & KI for the NanoCentury, Korea Advanced Institute of Science and Technology (KAIST), Daejeon 305-701, South Korea and [⊥]Hewlett-Packard (HP) Laboratory, Palo Alto, California 94304, United States. [¶]These authors contributed equally to this work.

Highly sensitive, fast-responding, and low-power hydrogen (H₂) sensors are in high demand for H₂ detection in a wide range of hydrogen-related application fields such as industrial processing, fuel cells, hydrogen storage and separation, etc.[1−4] Palladium (Pd) has been commonly used as H₂ sensing material with high sensitivity and selectivity. H₂ molecules can be selectively adsorbed onto the surface of Pd, dissociated into hydrogen atoms (H₂→2H), and diffused into the interstitial sites of Pd structures.[5] As a result, the resistance of Pd changes by the formation of a solid solution of Pd/H (α-phase) or a palladium hydride (β-phase). At room temperature and atmospheric pressure, the transition from α-phase to β-phase starts at 1−2% of H₂ concentrations, leading to an increase in lattice constant of 3.5%.[6]

Recently, one-dimensional (1D) Pd nanostructures such as nanowires and nanotubes[5,7−14] have shown great promise for use as the next generation sensor with high sensitivity, short response time, and ultra-low power consumption due to their large surface-to-volume ratio and high surface reactivity. Various approaches including electrodeposition of Pd at step-edge on graphite surface or into the nanochannels of anodic aluminum oxide (AAO) membranes,[7−10] lithographically patterned nanowire electrodeposition (LPNE) of Pd,[11−13] electron-beam lithography-based Pd nano-patterns,[14] and deposition and etching under angles (DEA)[5] have been developed and utilized to fabricate 1D Pd nanostructures for H₂ sensors with rapid response and high sensitivity. However, previously developed

methods have certain limitations for wide and practical applications of H₂ sensing. The fabrication of single Pd nanowires by electrodeposition on step-edges of graphite has poor reproducibility and production yields. Furthermore, a transfer process of nanowires from graphite to insulating substrate is needed.[7,8] Electrodeposition of Pd into

ABSTRACT

We developed a novel low-temperature, wet-chemical process for the facile synthesis of metal nanotube arrays through the reduction of metal precursors along sacrificial metal oxide nanowire templates and demonstrated its applications to the ultrasensitive, low-power, mechanically robust, and flexible chemical sensors. The *in situ* dissolution of ZnO nanowire templates, which were hydrothermally grown on electrode surfaces, during the reaction allows the direct formation of tubular Pd nanostructures on the sensor devices without the need of complex processes for device integration or template removal. Moreover, this simple synthesis was carried out at low-temperature with mild chemical conditions; therefore we could make Pd nanotube devices not only on silicon substrates but also on flexible polymer substrates. The H₂ sensing of such Pd nanotube devices was investigated under various mechanical loading and showed excellent reliability and robustness. The sensitivity of our devices was found to be at least 2 orders of magnitude higher than literature values for H₂ sensors, which can be attributed to the high surface area and the well-formed interconnect of Pd tubular nanostructures in our devices.

KEYWORDS: hydrogen sensor · flexible sensor · Pd nanotube · chemical sensing · ZnO nanowire
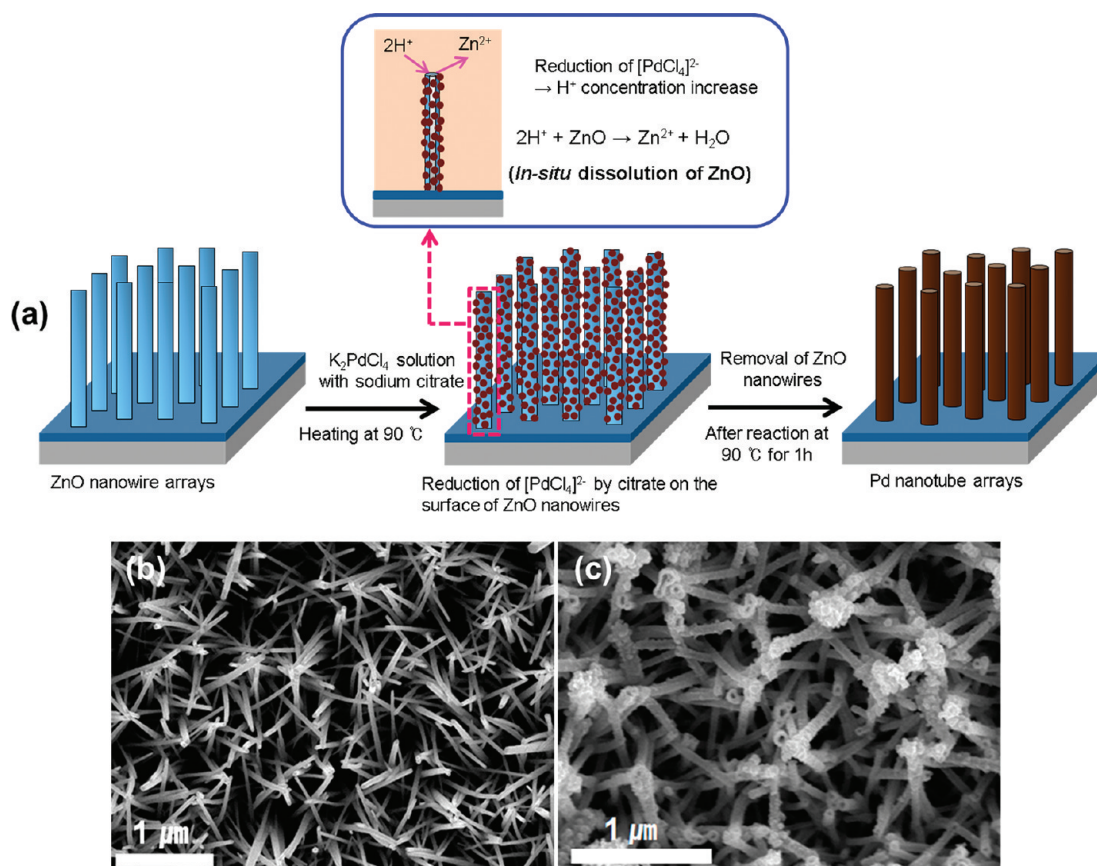
Figure 1. Synthesis of Pd nanotube array by low-temperature, wet-chemical process. (a) Schematic illustration showing the synthesis process of Pd nanotube arrays. SEM images of (b) ZnO nanowires and (c) Pd nanotube arrays. By using hydrothermally grown ZnO nanowires as sacrificial templates and the reduction of Pd precursor, Pd nanotubes can be fabricated rapidly with high yields and good uniformity. There are no additional processes required for the removal of templates through *in situ* dissolution of ZnO due to the reaction with H$^+$ ions generated by the reduction of the Pd precursor.

the nanochannels of AAO porous membranes requires additional processes to eliminate the porous membranes for the release of the nanostructures as well as to deposit a metal contact or interconnection layer.[9,10] E-beam lithography[14] requires expensive equipment for nanopatterning. Since the LPNE[11−13] method relies on the electrodeposition of metal precursor solution along the lithographically patterned and undercut-etched sacrificial Ni electrodes, the control of area number density, straightness, and line edge roughness of Pd nanowires is limited. Furthermore, a tight control of process parameters of electrochemical deposition is required to obtain desired dimension and morphology of nanowires. The DEA method[5] is based on the angled deposition and ion beam etching, causing the same problems (limited area number density, straightness, and line edge roughness) as the LPNE method and possible damage along the sidewalls of nanowires due to the lateral bombardment of ions during ion beam etching step. On the basis of these facts, development of simple, low-cost, and versatile techniques for the facile production of uniform 1D Pd nanostructures is highly required.

In this work, we have developed novel, highly sensitive, and low-power H$_2$ sensors based on Pd nanotube arrays that were synthesized by a facile chemical process, which involves the reduction of metal precursors with sodium citrate along the hydrothermally grown ZnO nanowire-based sacrificial templates. The formation of tubular nanostructures is attributed to the *in situ* dissolution of ZnO used as sacrificial templates during the reaction. Therefore, this method can lead to the direct formation of 1D Pd nanostructures on the substrate without additional processes to transfer Pd nanotubes to device substrate or to dissolve the ZnO nanowire-template after the reaction. Moreover, this simple synthesis is carried out under low-temperature and mild chemical condition, and thus allows the compatibility with flexible polymer substrates. We have demonstrated highly sensitive and flexible H$_2$ sensors based on Pd nanotube arrays for the first time by fabricating them on flexible polymer films. The H$_2$ sensitivity of Pd nanotube array-based sensors on flexible polyimide films and rigid silicon substrates is remarkably higher than those for previously reported H$_2$ sensors[5,13,15,16] due to high surface area of tubular nanostructures and well-interconnected structures of
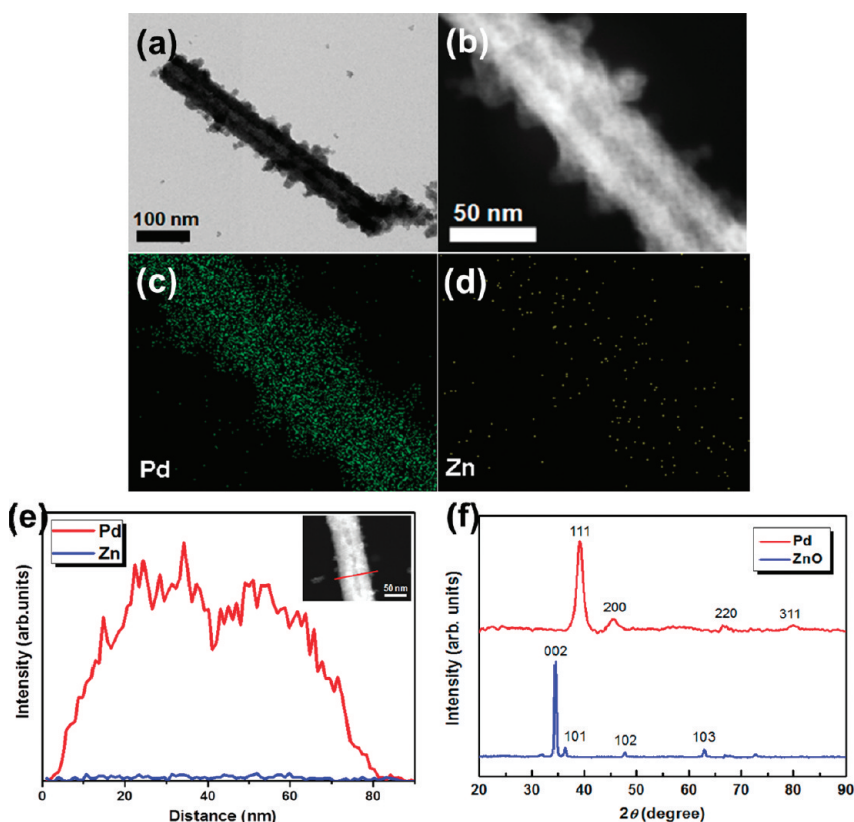
Figure 2. Material characterization of synthesized Pd nanotubes: (a) TEM image, (b—d) HAADF-STEM-EDS elemental mapping images, and (e) cross-sectional composition line profiles of a single Pd nanotube by EDS. Almost no traces of Zn is observed, proving the removal of ZnO nanowires and formation of Pd nanotubes. (f) XRD patterns of ZnO nanowires and Pd nanotubes. This XRD data also confirm that Pd nanoparticles were well crystallized along the ZnO nanowire templates while ZnO nanowires were etched away.

Pd nanotubes. In addition, the flexible H_2 sensors based on Pd nanotube arrays exhibited excellent mechanical bendability and durability. Therefore it is expected that these sensors would be extremely useful for the applications in various systems that demands highly sensitive chemical sensing with lightweight, mechanical flexibility, and robustness.

RESULTS AND DISCUSSION

The fabrication process of Pd nanotube arrays is illustrated in Figure 1a. The nanotubes were prepared by the reaction of the aqueous solution of Pd precursor containing sodium citrate and ZnO nanowires that were hydrothermally grown at 90 °C for 1 h based on the work of Yang et al.[17−19] In our previous work, an extremely simple and facile chemical process to synthesize uniform 1D metal nanotubes (Pt, Pd) was demonstrated for the first time using ZnO nanowires as sacrificial templates, with their applications to the flexible strain sensor and catalytic materials for proton exchange membrane fuel cells (PEMFCs).[21,22] The formation of hollow Pd nanotubes is attributed to the selective etching of ZnO nanowires by the increased acidity in the solution, which is due to the consumption of OH^- ions via the reduction of $PdCl_4^{2-}$ by citrate.[23]

Generally, it has been known that ZnO can be dissolved by a reaction with both H^+ and OH^- ions in acidic and alkaline solutions, respectively.[24,25] Therefore, Pd nanotubes could be prepared rapidly with high yields and good uniformity without a further removal process of the templates through in situ dissolution of ZnO due to the reaction with H^+ ions generated by the reduction of the Pd precursor. Figure 1 panels b and c show scanning electron microscopy (SEM) images of ZnO nanowires grown on a substrate by the hydrothermal synthesis method and Pd nanotubes synthesized using ZnO nanowire as sacrificial templates, respectively. The lengths of Pd nanotubes are almost identical to those of the ZnO nanowires (1−2 μm), while the diameters of the Pd nanotubes (50−100 nm) are generally larger than those of the ZnO nanowires (35−80 nm), which can be attributed to the deposition of Pd nanoparticles on the surface of ZnO nanowire-templates via the reduction of Pd precursor by citrate along with controlled etching of ZnO nanowires at the core. The shape of a Pd nanotube as a hollow structure was observed in transmission electron microscopy (TEM) images (Figure 2).

High-angle annular dark-field scanning TEM energy-dispersive X-ray spectroscopy (HAADF-STEM-EDS) mapping images of Pd and Zn (Figure 2a−d) and the
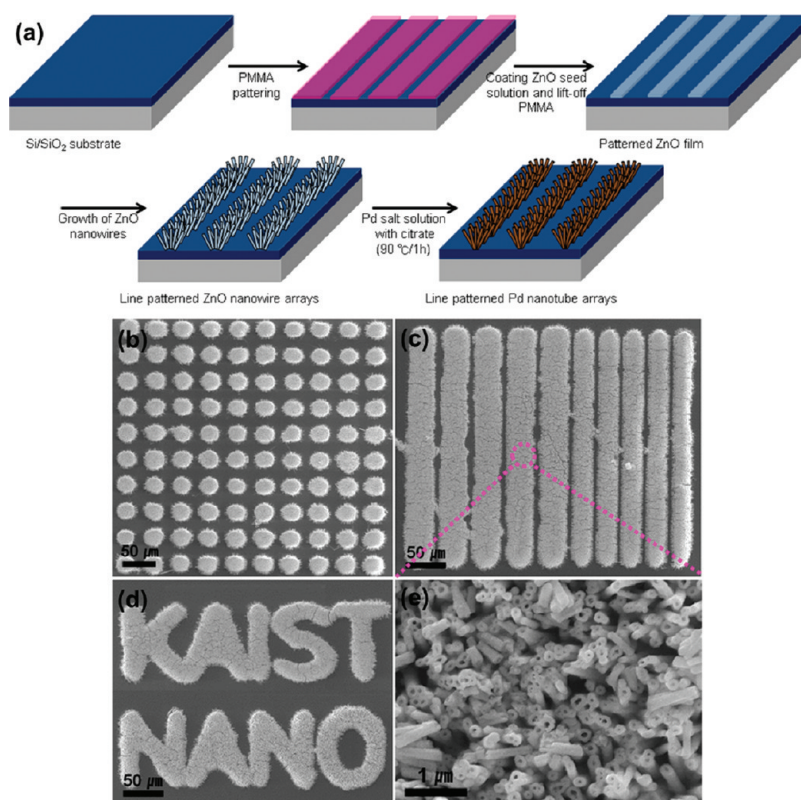
Figure 3. Patterned array of Pd nanotubes: (a) Fabrication procedure of a patterned array of Pd nanotubes. (b–d) SEM images of dot, line, and letter patterns of Pd nanotube arrays. (e) High-resolution SEM image of patterned Pd nanotube arrays. This result proves that our wet-chemical synthesis of Pd nanotubes by using sacrificial ZnO nanowire templates allows a simple method for the direct fabrication of a patterned array of Pd nanotubes on the device substrate.

compositional line profiles (Figure 2e) were measured on a single Pd nanotube. The results reveal that there is almost no trace of Zn, which is similar to that measured by inductively coupled plasma atomic emission spectrometer (ICP–AES) (Pd/Zn molar ratio = 95:5). Figure 2f shows the XRD pattern of fabricated Pd nanotubes in comparison with that of pure ZnO nanowires. Here, the diffraction peaks of Pd can be observed clearly and can be indexed to the face-centered cubic (fcc) phase. Sharp diffraction peaks of Pd and no traces of ZnO peaks indicate that Pd nanoparticles were well crystallized along the ZnO nanowire templates while ZnO nanowires were etched away.

By utilizing patterned growth of sacrificial ZnO nanowire templates, a patterned array of nanotubes is made possible as shown in Figure 3a. First, a dual layer of positive photoresist (PR)/PMMA was patterned by UV photolithography and oxygen (O$_2$) plasma etching. Second, the ZnO nanocrystal seed layer was drop casted several times, followed by the lift-off process. Then, ZnO nanowires were selectively grown on the ZnO nanoparticle patterns. Finally, a patterned array of Pd nanotubes could be simply fabricated by the aforementioned process. Figure 3 panels b–d shows SEM images of dot, line, and letter patterns of Pd nanotube arrays. Pd nanotubes were grown only on

selectively patterned areas, whereas they could not be found at other locations. The facile wet-chemical synthesis of Pd nanotubes by using sacrificial ZnO nanowire templates allows an extremely simple method for the direct fabrication of a patterned array of Pd nanotubes on the device substrate.

For the application to H$_2$ gas sensing, Pd nanotube arrays were fabricated on a silicon chip as shown in Figure 4a. As a first step, Cr/Au electrodes were fabricated *via* photolithography, e-beam evaporation, and a lift-off process on a silicon substrate with a 2 μm thick SiO$_2$ layer. To prepare ZnO nanowire arrays locally on interdigitated electrodes, the seed solution of ZnO nanoparticles was coated on the photoresist-patterned interdigitated electrodes. After the lift-off process of photoresist, ZnO nanowire arrays were grown by the hydrothermal process. For the detection of H$_2$ gas, a Pd nanotube array-sensor was fabricated by the facile chemical reaction of the Pd precursor solution along the ZnO nanowire templates grown on the interdigitated electrodes.

Figure 4b–d shows the photograph of a Pd nanotube array sensor fabricated on a silicon chip and SEM images of Pd nanotube arrays synthesized selectively on interdigitated electrodes. Pd nanotube arrays locally synthesized on the electrodes have hollow structures similar to those prepared on a bare Si/SiO$_2$
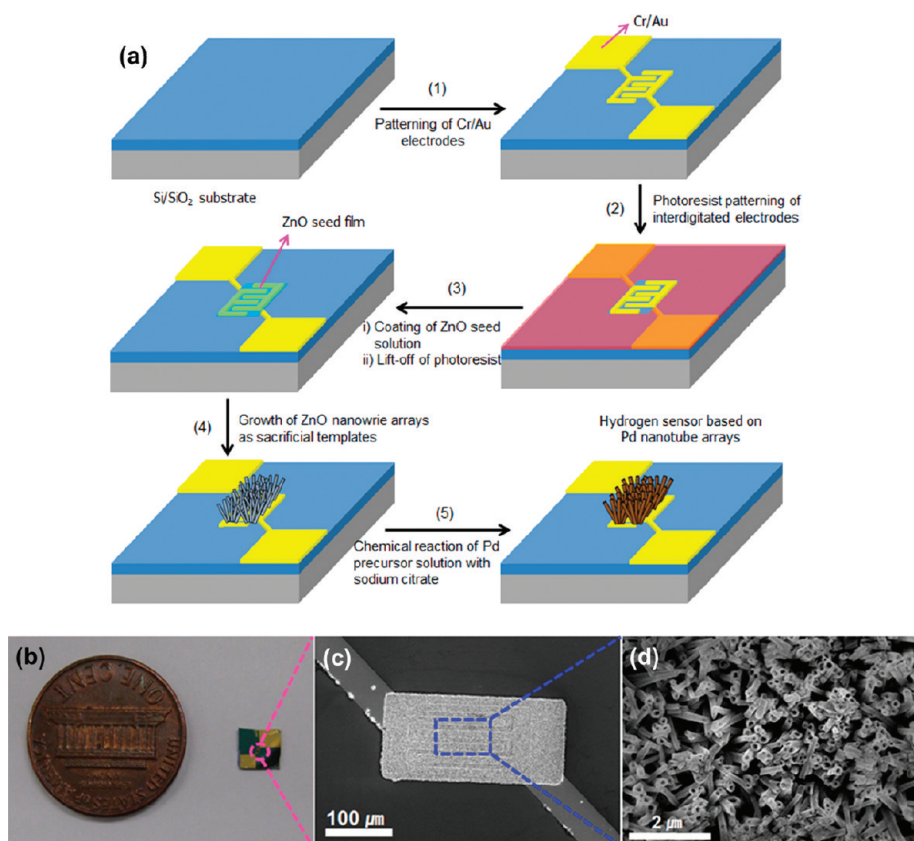
Figure 4. Fabrication of Pd nanotube sensor: (a) fabrication process of H$_2$ sensor based on Pd nanotube arrays; (b) photograph of a representative Pd nanotube array sensor; (c,d) SEM images of Pd nanotube arrays synthesized locally on interdigitated electrodes.

substrate shown in Figure 1c. This result indicates that the 1D metal nanostructures can be directly integrated on a chip by using our simple method through the self-elimination of the ZnO nanowire templates during the low-temperature reaction. Therefore, no additional integration processes such as removal of templates and/or transfer of nanomaterials from the synthesis substrates to the device substrates are required. Compared to the previously reported fabrication methods of nanomaterial-based sensors, this technique provides a much more facile route to the reliable and robust integration of nanomaterials on the sensor electrodes.

The current–voltage (I–V) characteristics were analyzed by using a semiconductor analyzer and temperature-controlled probe station. The current was measured while the voltage was swept from -2.0 to $+2.0$ V in the temperature range of 20–100 °C. In Figure 5a, a linear relation between current and voltage is observed, indicating that the Pd nanotube array behaves as an ohmic resistor. It is also observed that the electrical resistance is decreased at higher temperature. (e.g., $R = 7.9 \times 10^5$ Ω at $T = 20$ °C and $R = 1.6 \times 10^5$ Ω at $T = 100$ °C). The negative temperature dependence of electrical resistance can be attributed to the granular structure of Pd nanotubes. As shown in Figures 1c, 2a, and 2b, Pd nanotubes were synthesized by the as-

sembly of Pd nanoparticles along the sacrificial ZnO nanowire templates. Since discrete Pd nanoparticles are assembled in a granular form, a potential barrier to the intergrain flow of electrons is created and this results in the negative temperature coefficient of resistance.[26]

To investigate the H$_2$ sensing performance of Pd nanotube array sensor, the change of electrical resistance of sensor was measured during the exposure to H$_2$ gas with various concentrations (100–10,000 ppm) under room temperature conditions. The sensor response (S) was defined as the percentage of resistance change of the device by the exposure to H$_2$ gas.

$$S \% = (R_{H_2} - R_{air})/R_{air} \times 100 \qquad (1)$$

where R_{air} is the resistance of the sensor in the presence of air only and R_{H_2} is the resistances in the presence of H$_2$ at certain concentrations. The response time (τ) is defined as the time required for the sensor to reach 90% of the maximum resistance change after the sensor is exposed to a given concentration of H$_2$. Figure 5b shows the sensor response (S) vs time for the Pd nanotube sensor under different H$_2$ concentrations. The nanotube sensor could detect a wide range of H$_2$ concentrations with the increase of resistance. For example, the sensor showed a response of 247% and 3,754%
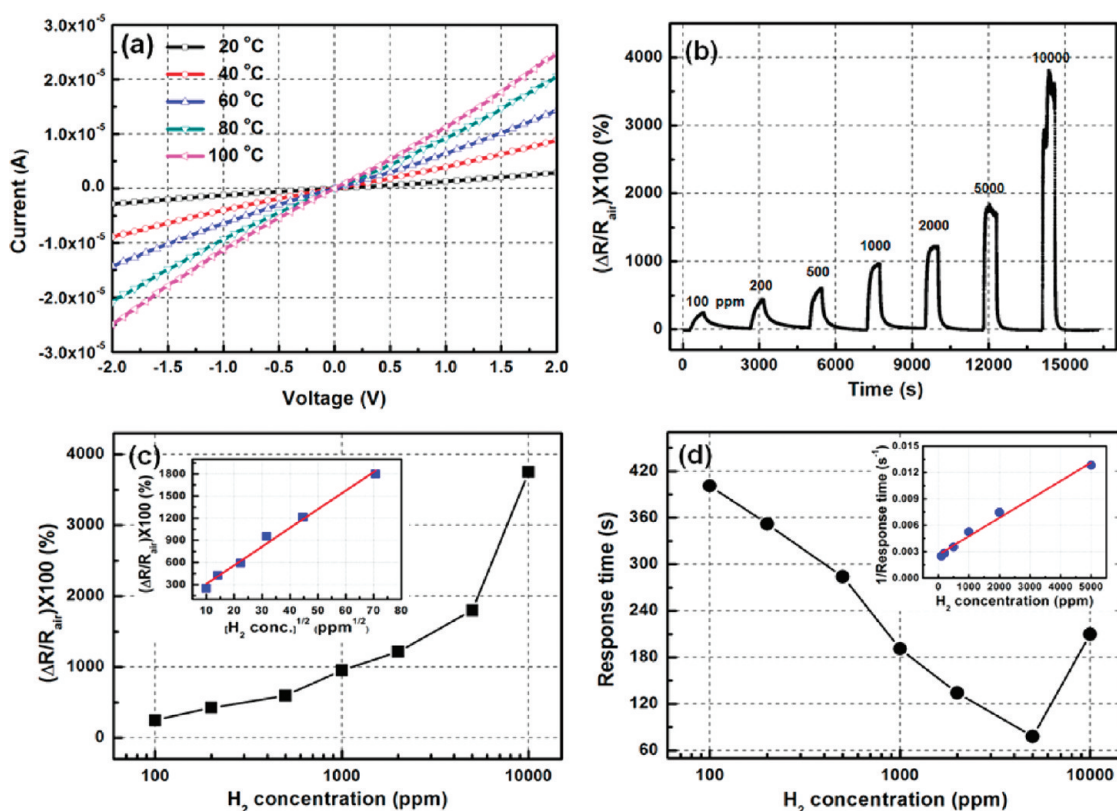
Figure 5. Device characterization of the Pd nanotube sensor: (a) current−voltage curve for fabricated Pd nanotube sensor at different temperatures (20−100 °C); (b) real-time response ($S = (\Delta R/R_{air}) \times 100$) of a Pd nanotube sensor under exposure to H_2 gas with various concentrations (100−10,000 ppm); (c,d) sensor response (S) and response time (τ) of a Pd nanotube sensor as a function of H_2 concentration. Insets of panels c and d show response (S) vs square root of H_2 concentration and response time ($1/\tau$) vs H_2 concentration.

to 100 ppm and 10,000 ppm of H_2 concentrations, respectively. The H_2 sensing mechanism in Pd nanostructures, which consist of well-connected Pd grains, is based on the increase of the electrical resistance by the adsorption of H_2 molecules.[27] H_2 molecules are adsorbed onto the surface of Pd and subsequently dissociated into hydrogen (H) atoms ($H_2 \rightarrow 2H$). Then, hydrogen atoms are diffused into the interstitial sites within the Pd lattice, producing α-phase of a solid solution in the case of low H_2 concentration (<1%). Conversely, at high H_2 concentration (>1%), diffused hydrogen atoms react with Pd atoms to form β-phase of palladium hydride (PdH_x) with a volume expansion of Pd lattice.[5,6] Therefore, the increase of resistance for our Pd nanotube sensor measured under various H_2 concentrations (100−10,000 ppm) can be attributed to the formation of α-phase by the exposure to H_2 gas.

Figure 5c shows that the response (S) of Pd nanotube sensor monotonically increases as the H_2 concentration is increased. The linear correlation between the sensitivity and the square root of H_2 concentration is observed at low H_2 concentration ($\leq$5,000 ppm) as indicated in the inset of Figure 5c. This can be understood with the Langmuir adsorption isotherm model considering that a H_2 molecule dissociates upon adsorption onto the Pd surface.[15,28] The H_2

dissociation reaction on Pd surface can be described as

$$H_2 + 2Pd \leftrightarrow 2PdH \qquad (2)$$

The adsorption rate of H_2 is $k_1 p_{H_2}(1 - \theta)^2$ and desorption rate is $k_{-1}\theta^2$, where k_1 and k_{-1} are the adsorption and desorption constant, respectively, p_{H_2} is the partial pressure of H_2, and θ is the fraction of Pd surface that is covered by H_2. At equilibrium, the adsorption rate equals the desorption rate:

$$k_1 p_{H_2}(1 - \theta)^2 = k_{-1}\theta^2$$
$$\rightarrow \theta/(1 - \theta) = (k_1/k_{-1})^{1/2} p_{H_2}^{1/2} \qquad (3)$$

For small θ in case of low partial pressure (i.e., low concentration) of H_2,

$$\theta \approx \theta/(1 - \theta) = (k_1/k_{-1})^{1/2} p_{H_2}^{1/2} \qquad (4)$$

Assuming that the resistance change ($\Delta R/R_{air}$) of sensor is proportional to θ for low H_2 concentration, the resistance change is proportional to the square root of the partial pressure and concentration of H_2 as follows.

$$\Delta R/R_{air} \propto (k_1/k_{-1})^{1/2} p_{H_2}^{1/2} \propto (k_1/k_{-1})^{1/2}[H_2]^{1/2} \qquad (5)$$

The H_2 sensitivity of our Pd nanotube array-based sensor is remarkably higher in comparison to those of

other 1D Pd nanostructure-based sensors reported in the literature. For example, Offermans et al.[5] reported the sensor response (S) of 3% for single 50−80 nm Pd nanowires, Rumiche et al.[15] reported S = 0.5−3% for Pd nanowire arrays, Yang et al.[13] reported S = 10−12% for Pd nanowires with the thickness of 11−94 nm and width of 33−183 nm, and Yu et al.[16] reported S = 11.6% for Pd nanotube membrane, all at 1% H_2 concentration. The response (S) of Pd nanotube sensor developed in this work was measured to be 3754% at 1% H_2 concentration as shown in Figure 5c. This value is 2−3 orders of magnitude higher than those of the aforementioned Pd nanowire and nanotube-based sensors.[5,13,15,16] It is presumed that the high sensitivity of Pd nanotube sensor to H_2 gas is due to the large surface area and high surface reactivity of tubular nanostructures as well as the well-formed interconnect among the Pd nanotube arrays.

The lowest detectable concentration was limited by the present experimental setup. However, we can derive the lowest detectable concentration of H_2 gas by extrapolating the curve fitting of data at higher concentrations into the lower concentration range and comparing that to the noise level. We took four data points (100, 200, 500, and 1,000 ppm) for plotting the response of the Pd NT sensor at a relatively low H_2 concentrations (≤1,000 ppm) and used a linear function for the curve fitting as shown in Figure S1 (Supporting Information). According to L. Peng et al.,[29] the limit of detection (LOD) can be calculated from the following equation:

$$LOD = 3\,(rms_{noise})/k \tag{6}$$

where k is the slope for the linear fit of the response and rms_{noise} is calculated as

$$rms_{noise} = \sqrt{\frac{V_{x^2}}{N}} \tag{7}$$

Here, N is the number of data points used for the average value and statistical parameter V_{x^2} is obtained from the following equation:

$$V_{x^2} = \sum (y_i - y)^2 \tag{8}$$

where y_i is the average value from calculation and y is the measured data point in the baseline (i.e., stable response before flowing H_2 gas). Using the above equations, the H_2 detection limit of our Pd nanotube sensor is calculated to be 1.3 ppm. This value is comparable or better than those of other Pd nanostructure-based H_2 sensors recently reported in the literature.[5,11−13] This low limit of detection can be also attributed to the large surface area, well-interconnected tubular structure of Pd nanotubes, and Pd nanoparticles constituting the granular structure of Pd nanotubes.

To investigate the hysteresis behavior and repeatability of the Pd nanotube sensor, we have conducted a repeatability test for the sensor after the exposure to 10,000 ppm. As shown in Figure S2 (Supporting Information), the sensor was exposed to alternating cycles of 100 ppm → 10,000 ppm → 100 ppm → 10,000 ppm → 100 ppm. The responses from this cycle were measured to be 211%, 4,100%, 190%, 3,973%, and 226%. From this test, it was found that the sensor is reversible even after the exposure to 10,000 ppm and provides a good repeatability.

The response time (τ) of the Pd nanotube sensor generally tends to be shortened (for $[H_2]$ = 100 ppm, τ = 400 s; for $[H_2]$ = 5,000 ppm, τ = 78 s) with the increase of H_2 concentration except for the concentration of 10,000 ppm as shown in Figure 5d. The response time for the 10,000 ppm was large (210 s) due to the unstable fluctuation of the sensor signal. This unstable fluctuation of signal at 10,000 ppm may be due to the very high resistance of Pd nanotubes and loss of stable ohmic contact between Pd nanotubes and Au electrodes by the solution of hydrogen in Pd nanotubes. The inverse of the response time (1/τ), which corresponds to the initial H_2 adsorption rate, follows a linear relationship with H_2 concentration (inset of Figure 5d). According to the Langmuir adsorption model, at the initial stage of measurement, the adsorption rate of H_2 is $r = k_1 p_{H_2}(1 - \theta)^2$. Since θ is negligible at the early stage, the adsorption rate is expected to be $r \approx k_1 p_{H_2} \propto k_1 [H_2]$. The response behavior of Pd nanotube array-based sensor is also consistent with the those of previously reported H_2 sensors made of Pd nanostructures (nanowires and nanotubes).[5,16]

The effect of temperature on the response to H_2 gas for the Pd nanotube sensor was investigated. Figure 6a shows the sensor response (S) to different H_2 concentrations at 100 °C. Compared to the response at 25 °C shown in Figure 5, both the sensitivity and response time are highly improved at 100 °C. As shown in Figure 6 panels b and c, the Pd nanotube sensor measured at 100 °C exhibited much shorter response time (τ = 27 s) as well as higher response (S = 6,866%) compared to those for 25 °C (τ = 78 s, S = 1,798%) during the exposure to H_2 gas at 5,000 ppm. The shorter response time can be explained by faster diffusion and dissociation of hydrogen at higher temperatures. Also, increased sensitivity can be attributed to higher surface reactivity and more active adsorption of H_2 molecules to Pd nanostructures at elevated temperatures.

It should be noted to the readers that the data presented above were taken from a single device. Since Pd nanotubes are fabricated in a bundle form by a sequential bottom-up chemical synthesis (synthesis of ZnO nanowires → assembly of Pd nanoparticles and in situ etching of sacrificial ZnO nanowire templates), their geometrical factors (diameter, length, number
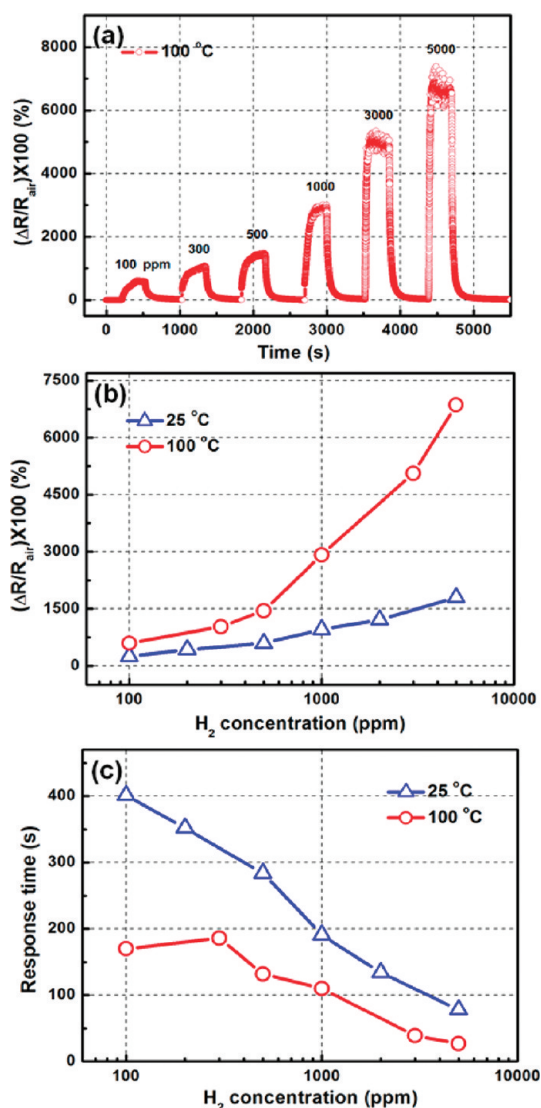
Figure 6. Temperature dependence of a Pd nanotube sensor: (a) real-time response ($S = (\Delta R/R_{air}) \times 100$) vs time, (b) response (S) vs H_2 concentration, and (c) response time (τ) vs H_2 concentration at 25 and 100 °C.
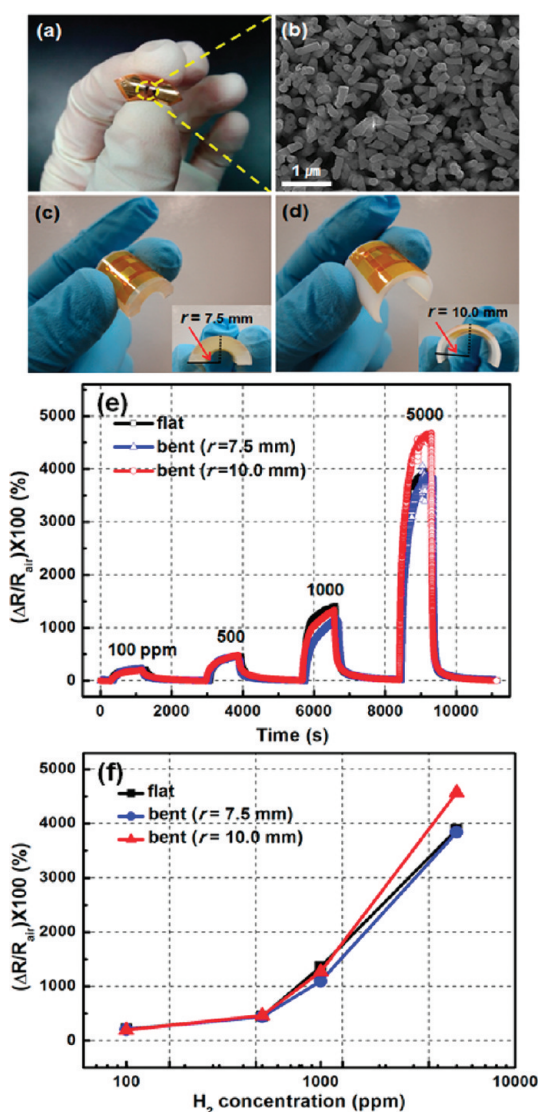

Figure 7. Flexible Pd nanotube sensor: (a) photograph of a flexible sensor based on Pd nanotube arrays; (b) SEM image of Pd nanotube arrays prepared on polyimide film; (c,d) photographs of flexible sensors attached on the cylindrical surface of silicone tubes with different radii (r = 7.5, 10.0 mm); (e,f) real-time response ($S = (\Delta R/R_{air}) \times 100$) vs time and response ($S$) vs H_2 concentration under various H_2 concentrations (100−5,000 ppm) with various curvature radii (ρ= 7.5 mm, 10.0 mm, and ∞).

density, and thickness of nanotubes) and electrical properties have a certain level of statistical variations. Therefore, their performance factors cannot be accurately controlled and consistent among different devices. A novel strategy for improving the control of geometrical and electrical parameters, and achieving much better performance consistency among different devices is currently being developed.

Recently, flexible sensors have attracted greater attention for their applications in various new areas such as hand-held, portable consumer electronics, aerospace science, and civil engineering that require biocompatibility, flexibility, lightweight, and mechanical shock-resistance.[30−32] Since our wet-chemical method allows facile synthesis and direct integration of Pd nanotubes in a benign chemical environment and low temperature conditions, it can also be applied

to the flexible polymer substrate. A flexible Pd nanotube array-based H_2 sensor could be easily fabricated on polyimide film as shown in Figure 7a,b. Further, the H_2 sensing capability of Pd nanotubes at low temperatures allows stable sensor operation on a polymer substrate. To characterize the mechanical flexibility of a Pd nanotube sensor for H_2 sensing, a bending experiment was carried out by laminating the sensors on the cylindrical surface of silicone tube with different diameters. Figure 7panels c and d show photographs of flexible sensors attached on the surface of silicone tubes with different radii of curvature of 7.5 and 10.0 mm, respectively. Figure 7 panels e and f present the
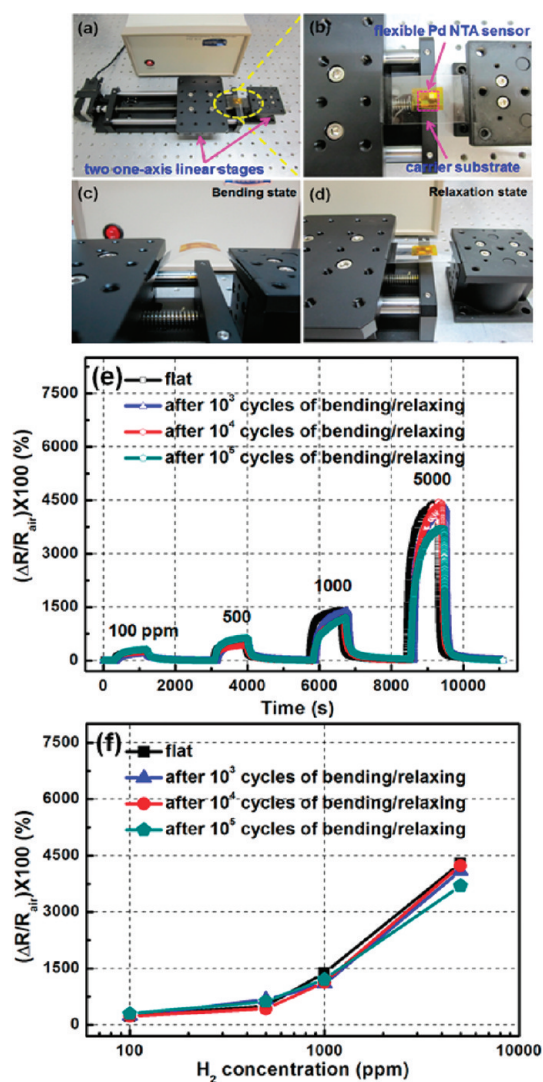
Figure 8. Mechanical robustness of a flexible Pd nanotube sensor under a cyclic bending condition: (a–d) experimental setup for fatigue test; (e,f) real-time response ($S = (\Delta R/R_{air}) \times 100$) vs time and response ($S$) vs H_2 concentration under various H_2 concentrations (100–5,000 ppm) after repeated bending between $\rho = 10.0$ mm and $\rho = \infty$ by 10^3–10^5 cycles.

response (S) of a flexible Pd nanotube sensor vs time and H_2 concentrations under various bending conditions (radii of curvature ρ = 7.5 mm, 10 mm, and ∞). The sensing results of the flexible Pd nanotube sensors are similar to the results of those fabricated on silicon chip. Compared to the sensitivity (sensor response S = 50–150%) of a flexible H_2 sensor based on a single wall carbon nanotube (SWCNT) decorated with Pd nanoparticles in the literature,[30,31] our sensor exhibits much higher sensitivity (sensor response S = 1,500%) for 0.1% H_2 concentration at room temperature. Moreover, the results show that bending the sensor did not affect the sensing performance significantly, except for the ∼18% increase of sensitivity for ρ = 10 mm compared with that for ρ = ∞ (flat condition) at $[H_2]$ = 5,000 ppm.

For the reliable operation of the flexible sensor device, robustness to bending conditions with not only positive curvature radii, but also negative curvature radii should be ensured. Therefore, we conducted a gas sensing test at a negative curvature of bending (ρ = −5.0 mm) as shown in Figure S3 (Supporting Information). From this test, we could find that the sensor response did not show any significant change in a large range of H_2 concentrations (100–5,000 ppm). The summary of responses of sensor to H_2 gas under various bending radii is presented in Table S1 (Supporting Information).

Additionally, the fatigue tests for the flexible Pd nanotube sensor were performed by using a pair of single-axis linear stages (see Figure 8a–d). Prior to the tests, a flexible sensor was mounted on the carrier substrate (polycarbonate film) and two ends of the carrier substrate were attached to a pair of single-axis linear stages. The bending and relaxation processes of the sensor were performed by the control of the distance between two linear stages with bending radii between ρ = 10.0 mm and ρ = ∞. Figure 8 panels e and f show the response (S) of the flexible Pd nanotube sensor to various H_2 concentrations (100–5,000 ppm) after bending and relaxing the sensor for 10^3–10^5 cycles, respectively. Although the sensitivity was reduced from the initial value at $[H_2]$ = 5,000 ppm by 15% after 10^5 cycles of bending, the sensitivity of the flexible sensor did not exhibit considerable change in general. These results indicate that the flexible Pd nanotube sensor fabricated on the polyimide film substrates via our facile chemical method exhibits excellent mechanical durability and robustness with no significant degradation of performance by static or repeated mechanical bending deformation. This excellent mechanical robustness can be attributed to the direct synthesis and in situ integration of Pd nanostructures on devices that allow superior physical binding and adhesion to the device electrodes and substrate.

CONCLUSION

In summary, we have developed a novel route toward the ultrasensitive and flexible gas sensors by using a low temperature wet-chemical synthesis of Pd nanotubes along ZnO nanowire-based sacrificial templates. The hollow structure of the Pd nanotube is attributed to in situ dissolution of ZnO nanowires by the reaction with H^+ ions that are generated in the solution during the reduction of the Pd precursor. Pd nanotube arrays could be directly synthesized and integrated in situ on flexible polymer substrate as well as silicon chip via this facile approach without additional integration processes. The sensors exhibit extremely high sensitivity compared with previously reported Pd nanostructure-based sensors by at least 2 orders of magnitude due to the large surface area and well-interconnected structures of Pd nanotubes.

Flexible Pd nanotube sensors fabricated on polyimide film show excellent mechanical bendability, durability, and robustness as well as excellent H_2 sensing performance. It is expected that our facile fabrication method of flexible H_2 sensors can be used in various engineering applications such as H_2 storage facilities, H_2 fueled vehicles, or space shuttles that require not only high sensitivity and fast response, but also lightweight, conformal wrapping on curved surfaces, and mechanical robustness.

METHODS

Synthesis of Pd Nanotubes. ZnO nanowire arrays were prepared on Si/SiO_2 substrates, by a similar method introduced by Yang et al.[17−19] In the first step, the ZnO nanoparticle (3−5 nm) solution was prepared based on the literature[20] to form the film of ZnO nanocrystal seeds. For the preparation of the solution, zinc acetate dihydrate (0.01 M) was dissolved in methanol (125 mL) under vigorous stirring at about 60 °C. Subsequently, a 0.03 M solution of KOH (65 mL) in methanol was added dropwise at 60 °C. The reaction mixture was stirred for 2 h at 60 °C. The substrates were coated with a droplet of ZnO nanoparticle dispersion, rinsed with ethanol, and then blow-dried with nitrogen gas. This step was repeated several times for a complete coverage of seeds, and the substrate was annealed at 150 °C for 20 min. ZnO nanowire arrays were then grown hydrothermally by immersing the seeded substrate in aqueous solutions containing zinc nitrate (25 mM), HMTA (25 mM), and PEI (6 mM) at 95 °C for 2.5 h. The substrate was then removed from the solution, washed with deionized water, and blow-dried.

For the synthesis of Pd nanotube arrays, Si/SiO_2 substrates grown with ZnO nanowires were fixed on the polytetrafluoroethylene (PTFE) holder and immersed in a container filled with a 3−4 mL of Pd precursor solution. The solution was prepared by adding sodium citrate solution (30 mM) into the aqueous solution of K_2PdCl_4 (5 mM). Sodium citrate was used as a reducing agent and a stabilizer. The container was closed and maintained at 90 °C for 1 h in a conventional convection oven. After the reaction, the samples were taken out and washed with triply distilled water and ethanol.

Material Characterization. Scanning electron microscopy (SEM) images of the samples were taken with a field-emission scanning electron microscope (FESEM, Phillips model XL30 FEG). Transmission electron microscopy (TEM) and high-angle annular dark-field scanning TEM (HAADF-STEM) characterization were performed with an FEI Tecnai G2 F30 Super-Twin transmission electron microscope operating at 300 kV. TEM samples were prepared after placing a drop of the aqueous dispersion of Pd nanotubes, which was obtained by sonication treatment of Pd nanotube arrays grown on Si/SiO_2 substrate, onto the carbon-coated copper grids (200 mesh). The effective electron probe size and dwell time used in HAADF-STEM-energy-dispersive X-ray spectroscopy (EDS) mapping experiments were 1.5 nm and 200 ms per pixel, respectively. The compositions of Pd and Zn in Pd nanotubes were quantified by inductively coupled plasma atomic emission spectrometer (ICP−AES, OPTIMA 330DV). X-ray diffraction (XRD) patterns were obtained with a Bruker AXS D8 DISCOVER diffractometer using Cu Kα (0.1542 nm) radiation.

Sensor Fabrication and Sensing Test. H_2 sensors based on Pd nanotube arrays were fabricated on thermally oxidized (t_{SiO_2} = 2 μm) silicon substrate and 75 μm thick flexible polyimide substrate. As a first step, interdigitated electrodes were fabricated via photolithography, e-beam evaporation of 200 nm thick Au thin film, and lift-off process. To promote the adhesion of Au, a thin Cr layer (10 nm thickness) was deposited before Au deposition. ZnO nanowire arrays were prepared locally on interdigitated electrodes by a hydrothermal method after seeding of the ZnO nanoparticles on the photopatterned substrates. For the detection of H_2 gas, Pd nanotube arrays were directly fabricated on the silicon and polyimide chips via the facile chemical process using Pd precursor solution and ZnO nanowire array templates as described previously. After the synthesis of Pd nanotubes, their electrical properties (i.e., I−V characteristics) were measured by using a semiconductor analyzer (HP 4155A) and temperature-controlled probe station.

Experimental setup for H_2 sensing consisted of a sealed chamber, mass flow controllers, DC power supply, and digital multimeters. The sensor chip was installed in a small test-chamber to which a gas inlet and outlet have been attached. Gas flow rate through the test chamber was controlled via mass flow controllers. The concentration of H_2 was controlled on the base of synthetic air consisting of N_2 (79%) and O_2 (21%) at atmospheric pressure. The flow rate was controlled at 1000 sccm throughout the test. The electrical response of the Pd nanotube-based sensor chip to H_2 gas was measured in real-time with a computer-controlled Keithley 197 digital multimeter. All data acquisitions were carried out with a LabView program through a GPIB interface card. To investigate the mechanical flexibility of a Pd nanotube array-based sensor fabricated on polyimide film, its H_2 sensing performance was measured through static bending tests with various radii of curvature and cyclic bending tests by repeating the bending/relaxing cycles at a frequency of 0.25 Hz for 10^3−10^5 times.

Supporting Information Available: Additional information and graphics as described in the text. This material is available free of charge via the Internet at http://pubs.acs.org.

REFERENCES AND NOTES

1. Kolmakov, A.; Klenov, D. O.; Lilach, Y.; Stemmer, S.; Moskovits, M. Enhanced Gas Sensing by Individual SnO_2 Nanowires and Nanobelts Functionalized with Pd Catalyst Particles. *Nano Lett.* **2005**, *5*, 667–673.

2. Nakagomi, S.; Okuda, K.; Kokubun, Y. Electrical Properties Dependent on H_2 Gas for New Structure Diode of Pt-Thin WO_3-SiC. *Sens. Actuators B* **2003**, *96*, 364–371.

3. Haryanto, A.; Fernando, S.; Murali, N.; Adhikari, S. Current Status of Hydrogen Production Techniques by Steam Reforming of Ethanol: A Review. *Energy Fuels* **2005**, *19*, 2098–2106.

4. Sun, Y.; Tao, Z.; Chen, J.; Herricks, T.; Xia, Y. Ag Nanowires Coated with Ag/Pd Alloy Sheaths and Their Use as Substrates for Reversible Absorption and Desorption of Hydrogen. *J. Am. Chem. Soc.* **2004**, *126*, 5940–5941.

5. Offermans, P.; Tong, H. D.; van Rijn, C. J. M.; Merken, P.; Brongersma, S. H.; Crego-Calama, M. Ultralow-Power Hydrogen Sensing with Single Palladium Nanowires. *Appl. Phys. Lett.* **2009**, *94*, 223110–223112.

6. Suleiman, M.; Jisrawi, N. M.; Dankert, O.; Reetz, M. T.; Bähtz, C.; Kirchheim, R.; Pundt, A. Phase Transition and Lattice Expansion during Hydrogen Loading of Nanometer Sized Palladium Clusters. *J. Alloys Compd.* **2003**, *356*, 644–648.

7. Favier, F.; Walter, E. C.; Zach, M. P.; Benter, T.; Penner, R. M. Hydrogen Sensors and Switches from Electrodeposited Palladium Mesowire Arrays. *Science* **2001**, *293*, 2227–2231.

8. Walter, E. C.; Favier, F.; Penner, R. M. Palladium Mesowire Arrays for Fast Hydrogen Sensors and Hydrogen-Actuated Switches. *Anal. Chem.* **2002**, *74*, 1546–1553.

9. Jeon, K. J.; Jeun, M.; Lee, E.; Lee, J. M.; Lee, K. I.; von Allmen, P.; Lee, W. Finite Size Effect on Hydrogen Gas Sensing Performance in Single Pd Nanowires. *Nanotechnology* **2008**, *19*, 495501–495506.

10. Cherevko, S.; Kulyk, N.; Fu, J.; Chung, C.-H. Hydrogen Sensing Performance of Electro-Deposited Conoidal Palladium Nanowire and Nanotube Arrays. *Sens. Actuators B* **2009**, *136*, 388–391.

11. Yang, F.; Taggart, D. K.; Penner, R. M. Fast, Sensitive Hydrogen Gas Detection Using Single Palladium Nanowires That Resist Fracture. *Nano Lett.* **2009**, *9*, 2177–2182.

12. Yang, F.; Taggart, D. K.; Penner, R. M. Joule Heating a Palladium Nanowire Sensor for Accelerated Response and Recovery to Hydrogen Gas. *Small* **2010**, *6*, 1422–1429.

13. Yang, F.; Kung, S.-C.; Cheng, M.; Hemminger, J. C.; Penner, R. M. Smaller is Faster and More Sensitive: The Effect of Wire Size on the Detection of Hydrogen by Single Palladium Nanowires. *ACS Nano* **2010**, *4*, 5233–5244.

14. Jeon, K. J.; Lee, J. M.; Lee, E.; Lee, W. Individual Pd Nanowire Hydrogen Sensors Fabricated by Electron-Beam Lithography. *Nanotechnology* **2009**, *20*, 135502–135507.

15. Rumiche, F.; Wang, H. H.; Hu, W. S.; Indacochea, J. E.; Wang, M. L. Anodized Aluminum Oxide (AAO) Nanowell Sensors for Hydrogen Detection. *Sens. Actuators B* **2008**, *134*, 869–877.

16. Yu, S.; Welp, U.; Hua, L. Z.; Rydh, A.; Kwok, W. K.; Wang, H. H. Fabrication of Palladium Nanotubes and Their Application in Hydrogen Sensing. *Chem. Mater.* **2005**, *17*, 3445–3450.

17. Greene, L. E.; Law, M.; Goldberger, J.; Kim, F.; Johnson, J. C.; Zhang, Y.; Saykall, R. J.; Yang, P. D. Low-Temperature Wafer-Scale Production of ZnO Nanowire Arrays. *Angew. Chem., Int. Ed.* **2003**, *42*, 3031–3034.

18. Law, M.; Greene, L. E.; Johnson, J. C.; Saykally, R. J.; Yang, P. D. Nanowire Dye-Sensitized Solar Cells. *Nat. Mater.* **2005**, *4*, 455–459.

19. Greene, L. E.; Yuhas, B. D.; Law, M.; Zitoun, D.; Yang, P. D. Solution-Grown Zinc Oxide Nanowires. *Inorg. Chem.* **2006**, *45*, 7535–7543.

20. Pacholski, C.; Komowski, A.; Weller, H. Self-Assembly of ZnO: From Nanodots to Nanorods. *Angew. Chem., Int. Ed.* **2002**, *41*, 1188–1191.

21. Lim, M. A.; Lee, Y. W.; Han, S. W.; Park, I. Novel Fabrication Method of Diverse One-Dimensional Pt/ZnO Hybrid Nanostructures and Its Sensor Application. *Nanotechnology* **2011**, *22*, 035601–035608.

22. Lee, Y. W.; Lim, M. A.; Kang, S. W.; Park, I.; Han, S. W. Facile Synthesis of Noble Metal Nanotubes by Using ZnO Nanowires as Sacrificial Scaffolds and Their Electrocatalytic Properties. *Chem. Commun.* **2011**, *47*, 6299–6301.

23. Jiménez, I. O.; Romero, F. M.; Bastús, N. G.; Puntes, V. Small Gold Nanoparticles Synthesized with Sodium Citrate and Heavy Water: Insights into the Reaction Mechanism. *J. Phys.Chem. C* **2010**, *114*, 1800–1804.

24. Willander, M.; Klason, P.; Yang, L. L.; Al-Hilli, S. M.; Zhao, Q. X.; Nur, O. ZnO Nanowires: Chemical Growth, Electrodeposition, and Application to Intracellular Nanosensors. *Phys. Status Solidi C* **2008**, *5*, 3076–3083.

25. She, G. W.; Zhang, X. H.; Shi, W. S.; Fan, X.; Chang, J. C.; Lee, C. S.; Lee, S. T.; Liu, C. H. Controlled Synthesis of Oriented Single-Crystal ZnO Nanotube Arrays on Transparent Conductive Substrates. *Appl. Phys. Lett.* **2008**, *92*, 053111–053113.

26. Feldman, C. J. Temperature Dependency of Resistance of Thin Metal Films. *Appl. Phys.* **1963**, *34*, 1710–1714.

27. Khanuja, M.; Varandani, D.; Mehta, B. R. Pulse Like Hydrogen Sensing Response in Pd Nanoparticle Layers. *Appl. Phys. Lett.* **2007**, *91*, 253121–253123.

28. Laidler, K. J. *Chemical Kinetics*; McGraw-Hill: New York, 1965; pp 260.

29. Peng, L.; Zhao, Q.; Wang, D.; Zhai, J.; Wang, P.; Pang, S.; Xie, T. Ultraviolet-Assisted Gas Sensing: A Potential Formaldehyde Detection Approach at Room Temperature Based on Zinc Oxide Nanorods. *Sens. Actuators B* **2009**, *136*, 80–85.

30. Sun, Y.; Hau Wang, H. High-Performance, Flexible Hydrogen Sensors That Use Carbon Nanotubes Decorated with Palladium Nanoparticles. *Adv. Mater.* **2007**, *19*, 2818–2823.

31. Sun, Y.; Hau Wang, H.; Xia, M. Single-Walled Carbon Nanotubes Modified with Pd Nanoparticles: Unique Building Blocks for High-Performance, Flexible Hydrogen Sensors. *J. Phys. Chem. C* **2008**, *112*, 1250–1259.

32. Mcalpine, M. C.; Ahmad, H.; Wang, D.; Heath, J. R. Highly Ordered Nanowire Arrays on Plastic Substrates for Ultrasensitive Flexible Chemical Sensors. *Nat. Mater.* **2007**, *6*, 379–384.